

Contents

1. Introduction	829
2. Description of the Various Types of Anomalies	831
3. Correlation With Ground Based Geomagnetic Activity Indices	832
4. Seasonal and Local Time Correlations	837
5. Correlation With the Day of the Week	841
6. Long Term and Progressive Effects	843
7. Summary and Conclusions	846
Acknowledgments	847
References	847
Appendix A	849

10. Spacecraft Charging Anomalies on the DSCS II, Launch 2 Satellites

George T. Inouye
TRW Defense and Space Systems Group
Redondo Beach, Calif.

Abstract

Six different types of anomalous events have occurred on two DSCS II satellites. The total number of events, over 100, and the long operational period, nearly 3 years, permits some statistical analyses to be performed. Correlation of occurrences of particular types of anomalies with equinoxes and seasons of the year are consistent with a spacecraft charging model. On the other hand, an interesting correlation of occurrences with days of the week has been found. Finally, a long term diminution in the frequency of occurrence of events has been observed, and is discussed in terms of environmental activity, material degradations and the need for more data.

1. INTRODUCTION

The DSCS II Launch 2 satellites, 8433 and 9434, were launched on 13 December 1973 and nearly 3 years of operational data are now available for these two geosynchronous orbit spacecraft. Figure 1 shows the longitudes of the two satellites from initial orbit insertion to final operating positions, one over the Atlantic and the other over the Pacific Ocean. Also shown are the occurrences of the anomalous events during the first few months. Over the 33 month period since launch, over

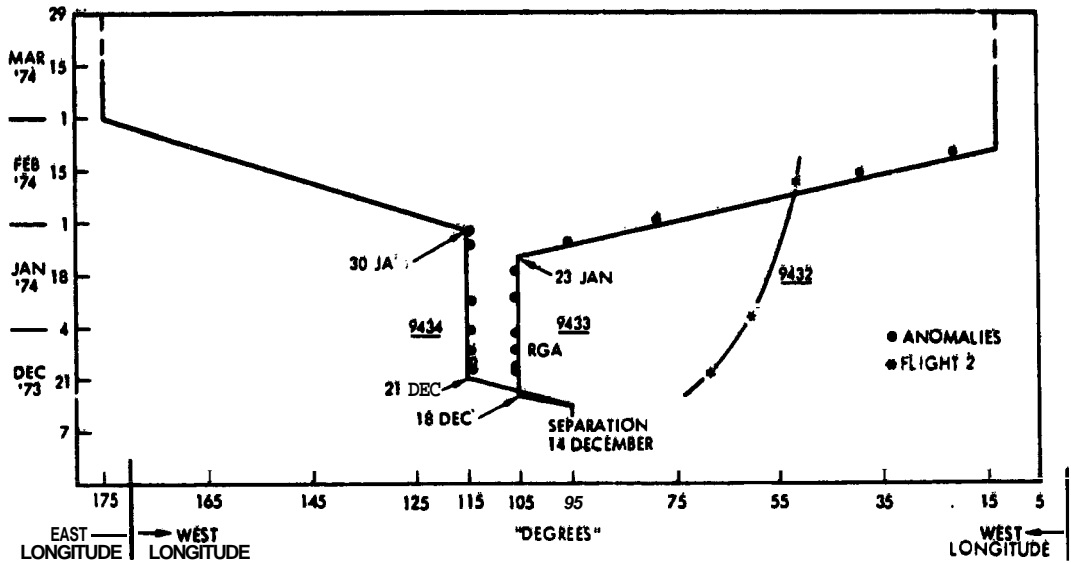


Figure 1. 943319434 Orbital Position

166 anomalous events have been observed. These events, rather than being of a single type, have been manifested in six different types of anomalies occurring in different locations on the spacecraft as well as in affecting different operating circuits at these locations.

The conclusions to be drawn from the results to be presented in this paper are that much further work, both in the Laboratory and in orbit, needs to be performed in the areas of spacecraft design and immunity verification testing. Studies that should be implemented run the gamut of materials' characterizations to analysis and test of specific spacecraft configurations. Finally, simplified in-flight monitoring of charging/discharging in the housekeeping telemetry of all geosynchronous satellites would serve as an invaluable diagnostic in the eventuality that anomalous events do occur. Our experience on the DSCS satellites has been that a great deal of effort was required to identify the sources of anomalous behavior, whether internal or due to the ambient environment.¹⁻⁷ In the final analysis, in spite of concentrated "detective work," some of the conclusions that the environment was the most likely causative source were arrived at by an elimination process rather than by a more direct approach because of the lack of diagnostic data.

2. DESCRIPTION OF THE VARIOUS TYPES OF ANOMALIES

The first type of anomalous behavior, the anomalous firing of the reset generator assembly (RGA upsets), was evidenced on the Launch 1 pair of satellites. Analysis of these events by Fredricks and Scarf⁸ led to the first realization that these events were related to the hot plasma environment of the geosynchronous orbit rather than to any internal malfunction within the spacecraft itself. Once identified, these anomalies were eliminated on the Launch 2 payloads by appropriate redesign except for a single recurrence which can be accounted for by the galactic cosmic ray environment. Figure 2 is an exploded cut-away view of the spacecraft. On top is the despun section containing the communications antenna array and most of the associated electrical hardware. "Despinning" permits the antennas to be continuously pointed towards the earth while the main spinning portion provides attitude stability. The spin axis is oriented to be parallel to the earth's polar rotational axis. The cylindrical outer shell of the spinning section is covered in with solar cells in eight sections or panels. On the spinning platform are located the supportive electrical hardware such as the power conditioning, housekeeping telemetry, and attitude control subsystems. The RGA associated circuitry is also located on the spinning platform.

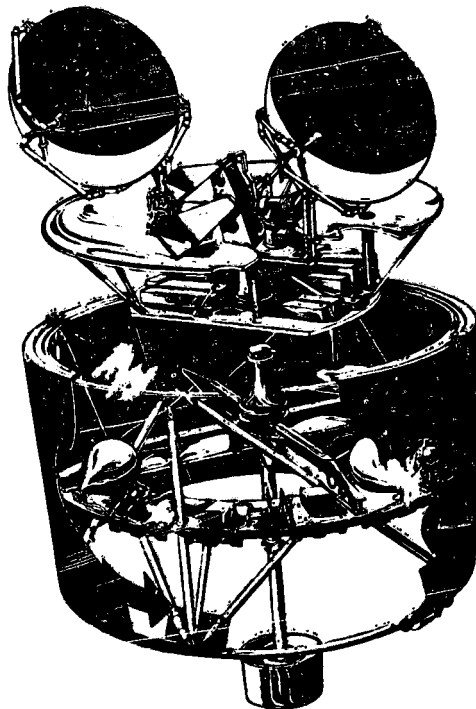


Figure 2. DSCS II Configuration

With the despin platform in place, the only access paths for ambient plasma and sunlight into the spinning platform cavity are the annular opening on the between the spinning and despin sections, eight slits between solar array panels, and portholes used for sensors and for attitude control thrusters in four of the solar array panels. The pressure transducer which failed during the first equinox season on Flight 4 (9434) is also located on the spinning platform as is the hardware associated with the spin type anomalies ("S"). The "S" events are also equinox related. All of the remaining types of anomalies, the anomalous activation of the Tunnel Diode Amplifier Logic, power converter switching and gimbal reset (the "T," "C" and Gimbal anomalies) are associated with circuits contained in an electronic unit located on the upper despin platform.

All of the anomalous behavior observed, aside from that of the pressure transducer, were the result of the upsetting of the state of bistable logic circuits, flip-flops, which could be caused by arc discharges in the near vicinity of the relevant electrical hardware. The ability of simulated arc discharges to cause all of the observed varieties of logic upsets has been demonstrated on a prototype (qualification model) spacecraft. It has been demonstrated that it is the coupling of arc discharges to the lines entering the various electronic boxes via the connector which causes the logic circuit upsets rather than any electromagnetic signals entering through the walls of the boxes. In the case of the pressure transducer, it was determined that nearby arc discharges could cause its failure in the manner observed in orbit. The failure mode is one in which the sensor does not recover, and therefore occurs only as a one-time event.

Of all of the various types of anomalies, the "S" were the potentially most serious, having to do with the spacecraft spin or despin rate control. After the fourth S-event, false command countermeasures were instituted. Thus, the problem was solved operationally, but at the same time the solution eliminated the possibility of obtaining additional data of the type discussed here.

3. CORRELATION WITH GROUND BASED GEOMAGNETIC ACTIVITY INDICES

The geomagnetic activity indices, the daily A-index from Anchorage, Alaska and Fredericksburg, Virginia are the most easily accessible measure of disturbances in the geomagnetic field. The relationship between geomagnetic substorms, the resulting hot plasma environment at synchronous orbit altitudes, and ground-based measurements is a subject of current research. Figures 3-5 are plots of these A-indices over the 33 month period from launch to the present. The occurrence of anomalous events are shown at the top of these figures with a 24 hr vertical scale of local time. The type of anomaly and spacecraft, 9433 or 9434, are

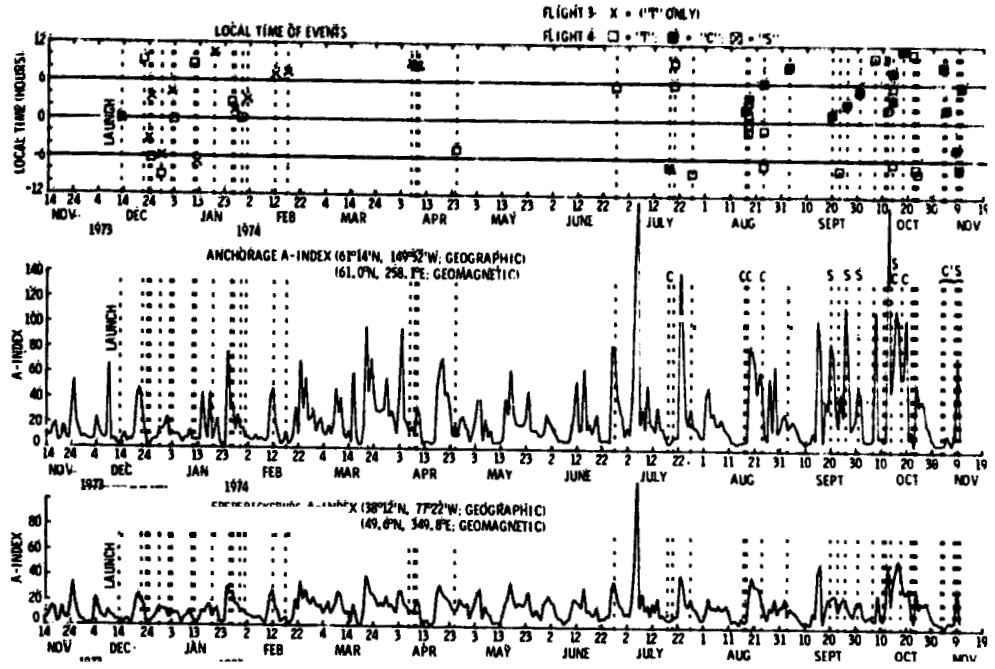


Figure 3. Timing of Events on Flights 3 and 4 and the Daily A-Indices From Fredericksburg and Anchorage For 1974

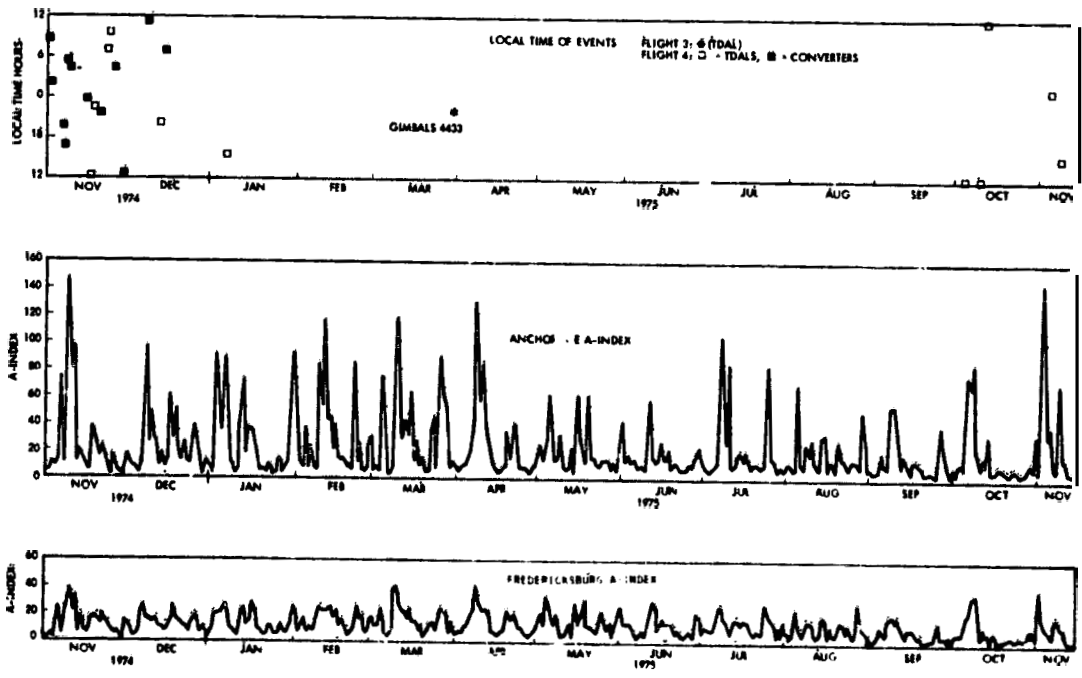


Figure 4. Timing of Events on Flights 3 and 4 and the Daily A-Indices: From Fredericksburg and Anchorage for 1975

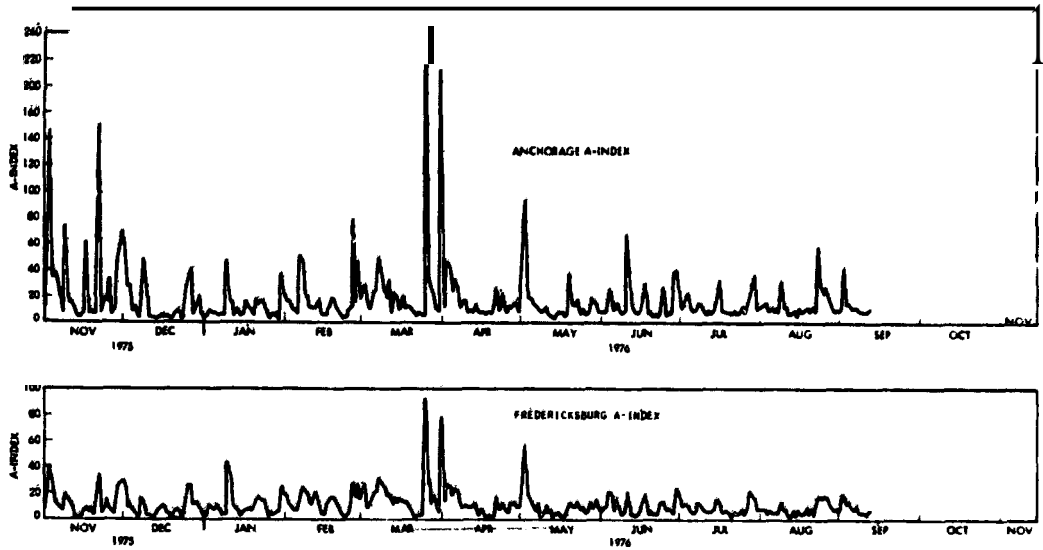


Figure 5. Timing of Events on Flights 3 and 4 and the Daily A-Indices From Fredericksburg and Anchorage for 1976

identified. All of the events are listed with greater detail in tabular form in Appendix A. The following features are most prominent in Figures 3-5:

- (1) There is no obvious correlation of event occurrences with the A-Indices.
- (2) The rate at which anomalies occur decreases with time.
- (3) There are no obvious preferred local times of occurrence.

The first feature, which is the subject of this section, will be discussed now and the other points will be discussed in following sections.

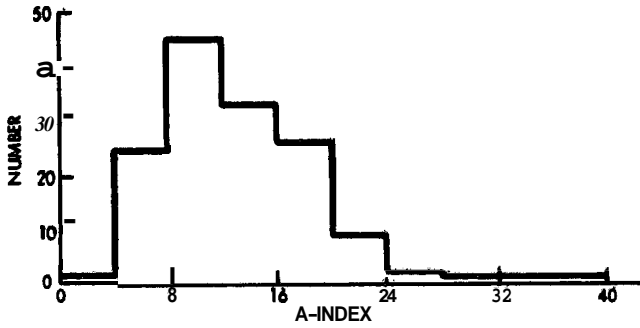
The Fredericksburg A-Index generally shows a lesser variability as well as smaller magnitudes as compared to the Anchorage index. We may surmise that if the latter station, which is more closely related to the geosynchronous orbit, had been located exactly at the "footprint" of the geomagnetic field line passing through one of the satellite positions, a much better correlation with the occurrence of anomalies would have been obtained. It should be noted, however, that the ground position of the footprint associated with a particular geosynchronous longitude is subject to large seasonal and geomagnetic storm induced variations because the geosynchronous altitude is close to the magnetospheric boundary. Geomagnetic substorms, with which the presence of hot plasma and the dearth of cold plasma is associated, are generally short-lived (approximately 0.1-1.0 hr), and are localized in longitude as well as in latitude or altitude. Being located at a lower latitude, the Fredericksburg station's A-Index should be expected to give a better

Indication of geomagnetic activity over all longitudes. It is for this reason that this index is used in the following statistical analyses.

Figure 6(a) shows the number of times that each value of A-Index at Fredericksburg occurred during the 33 month period. Each consecutive 7 day period was averaged to give a single data point, and the A-Index resolution was limited to multiples of four. Figure 6(b) shows the number of anomalies, which occurred in each A-Index group. Figure 6(c) is a histogram of Figure 6(b) divided by Figure 6(a) for each A-group, giving a corrected anomaly distribution which would be obtained if the A-Indices had been equally probable rather than as in Figure 6(a). Figure 6(c) shows a generally increasing trend in which the number of anomalies increased with the A-Index. The bars in Figure 6(c) have been broken down to show the individual contributions of the "T," "C" and "S" type anomalies. The figure does not show any dramatic threshold effect except for the "S" anomalies. The fact that a significant number of events occurred at low A-Index values (4 to 8) is a convincing argument for not pursuing the correlation further in such a crude manner.

Inspection of Figure 3 for the "S" anomalies which occurred in 1974 show that all four of these events did occur on A-Index peaks. Why they occurred on only one spacecraft and only in the fall equinox is not clear. This question of why events occurring on one spacecraft are not correlated with those on the other is unanswered. One possibility is the existence of configurational differences in the sense of spacecraft charging, (grounding of thermal blankets, thickness of vacuum deposited aluminum) of two spacecraft which are ostensibly identical. The other possibility is that there is a statistical variation in geosynchronous orbit environments. Figure 7 shows the geomagnetic latitude variation with geographic longitude. Spacecraft 9434 is at -5° South and 9433 is at $+6.5^{\circ}$ North. The two spacecraft are located at slightly different L, B points. Lyans et al,⁹ for example, show that energetic particle populations and their pitch angle distributions are expected to vary greatly with magnetic L, B values.

a) DISTRIBUTION OF DAILY A-INDEX OCCURRENCES



b) DISTRIBUTION OF ANOMALIES VS A-INDEX



c) (a) DIVIDED BY (b)

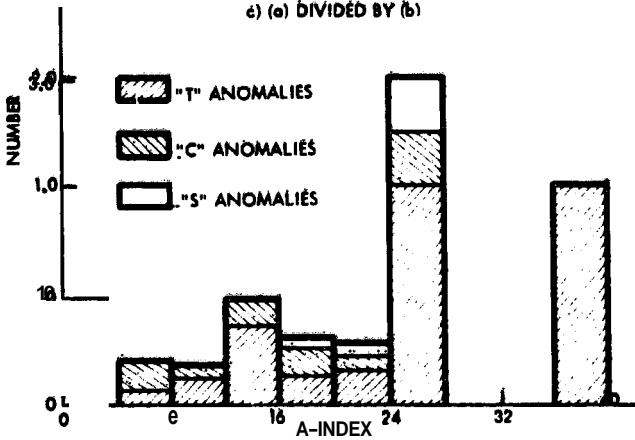


Figure 6. Distributions of Anomalies Versus Fredericksburg A-Index (7-day Averages)

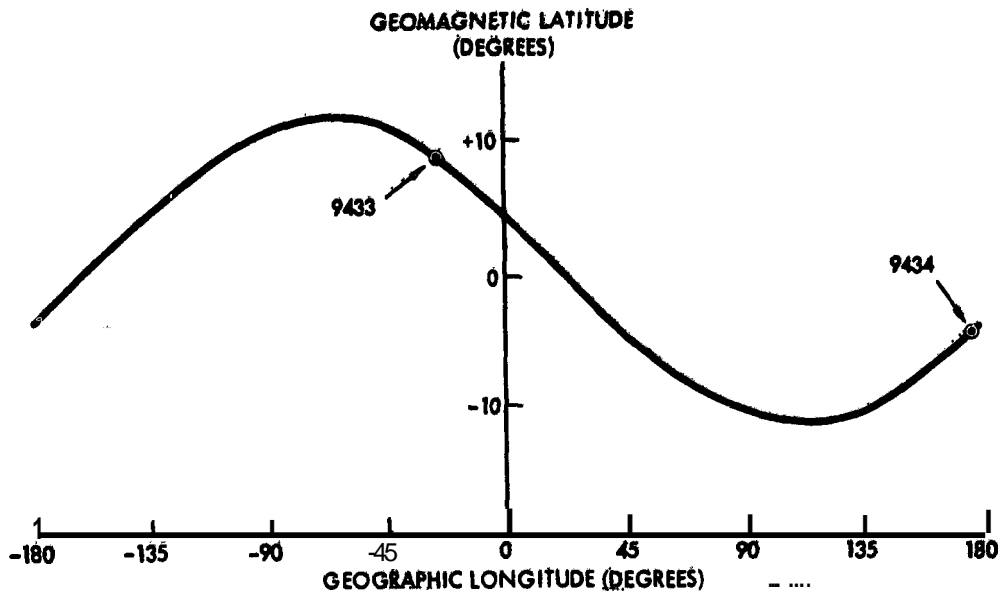


Figure 7. Geosynchronous Orbit Magnetic Latitude Versus Geographic Longitude

1. SEASONAL AND LOCAL TIME CORRELATIONS

As mentioned previously, "S" anomalies have been internally countermanded so that they cannot occur since the fall of 1974. Both the "S" anomalies during the fall equinox and the pressure transducer failure on spacecraft 9434 during the spring equinox of 1974 are consistent with the author's¹⁰ charging model prediction of a large negative spacecraft ground potential during the equinox when the metallic surface area of the spacecraft exposed to sunlight is at a minimum as shown in Figure 8(a). From Figure 3 for 1974 it may be seen that a 49 day period from February 11 to April 7 had no "T" anomalies. During the 1974 fall equinox season a similar period of 39 days lasted from August 24 to October 2 except for a single event on September 23. "C" type anomalies did not begin until July 20 and stopped occurring on December 15, 1974. This type of anomaly has been shown to be more nearly attributable to internal causes than any of the others.⁵ Here also, however, a 41 day period from September 3 to October 14 is void of these anomalies. Of the total of nine anomalies occurring during 1975, the two "Gimbal" anomalies occurred on March 12 and 14, and a "T" anomaly on March 31. These three events would tend to invalidate the equinox arguments from the charging model analysis, although the total number of events is much smaller than for the first year. During 1976 not a single anomaly has been observed so far.

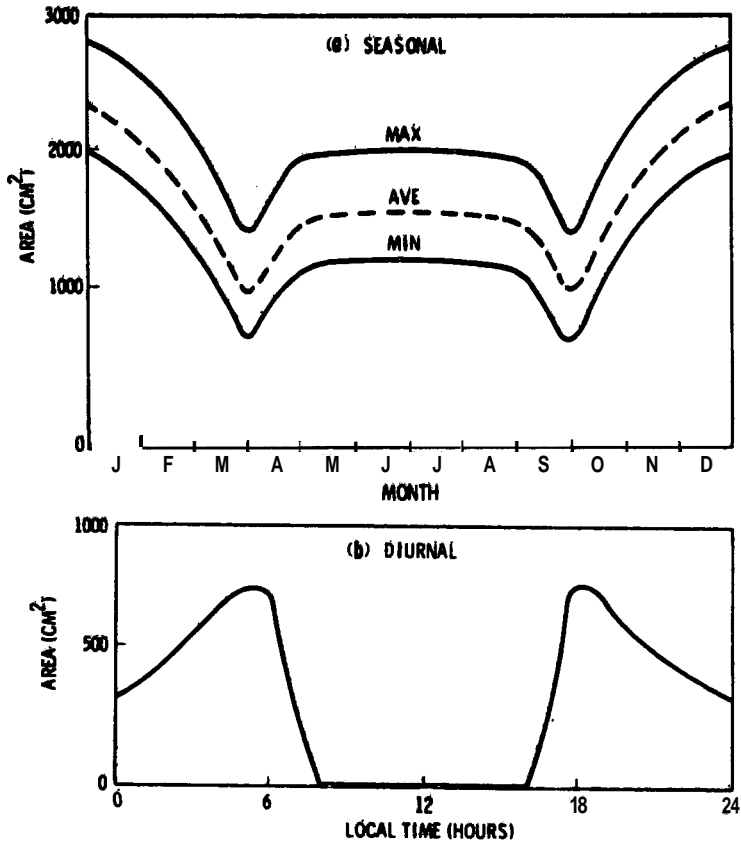


Figure 8. Seasonal and Diurnal Variation of Metallic Surface Areas Exposed to Sunlight

The comparison of the timing of anomalous events with local time may be examined in Figure 9. The results published by Fredricks and Scarf on the analysis of anomalous events on the Launch 1 DSCS satellites showed an excellent correlation (19 out of 23 events) with geomagnetic substorms. In particular the occurrence of anomalies during the midnight/dawn sector of local time was very convincing evidence of an environmental origin. "C" anomalies occurring within an hour of any initial event have been eliminated in the statistics. This accounts for the fewer number of events plotted in Figure 10 than are listed in the Appendix. The four "S" anomalies, as in their A-Index correlation with expected behavior, seem to meet the test of occurring during the midnight/dawn local time sector. The "T" and "C" anomaly distributions do not meet this test although the midnight/dawn sector seems to be somewhat more favored, particularly with the "C" anomalies. The most prominent features of the "T" anomaly distribution are a

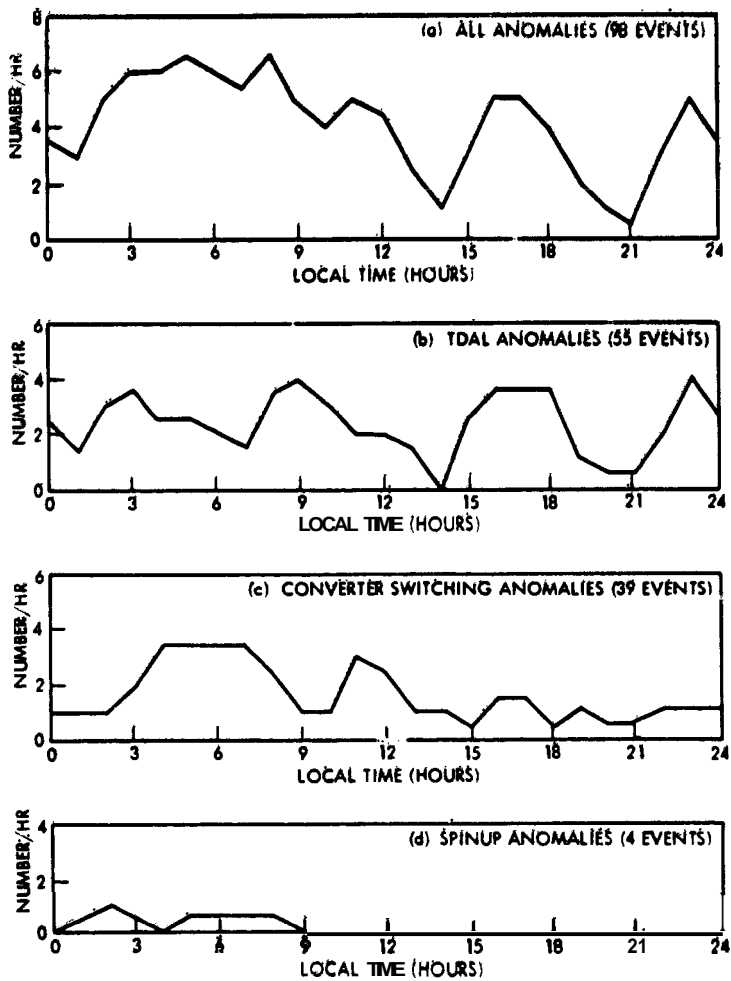


Figure 9. Distribution of Anomalous Events on DSCS in Local Time

fairly deep minimum near local noon and slightly enhanced peaks or "wings" a few hours before and after the dip. Figure 8(b) which shows the diurnal variation of the spacecraft metallic surface area exposed to sunlight also has these features. The minimum around local noon occurs when the despun antenna array is pointed away from the sun, and the dawn and dusk maxima occur when the sunlight impinges broadside on the six waveguide struts in front of the two large dish antennas. At local midnight the sunlight hits the waveguides directly on the narrower of its two cross-sectional dimensions. The maximum/minimum lines on Figure 8(a) for the seasonal variation represent the excursions due to the diurnal variation. The latter is a significant fraction of the former, especially during the equinoxes.

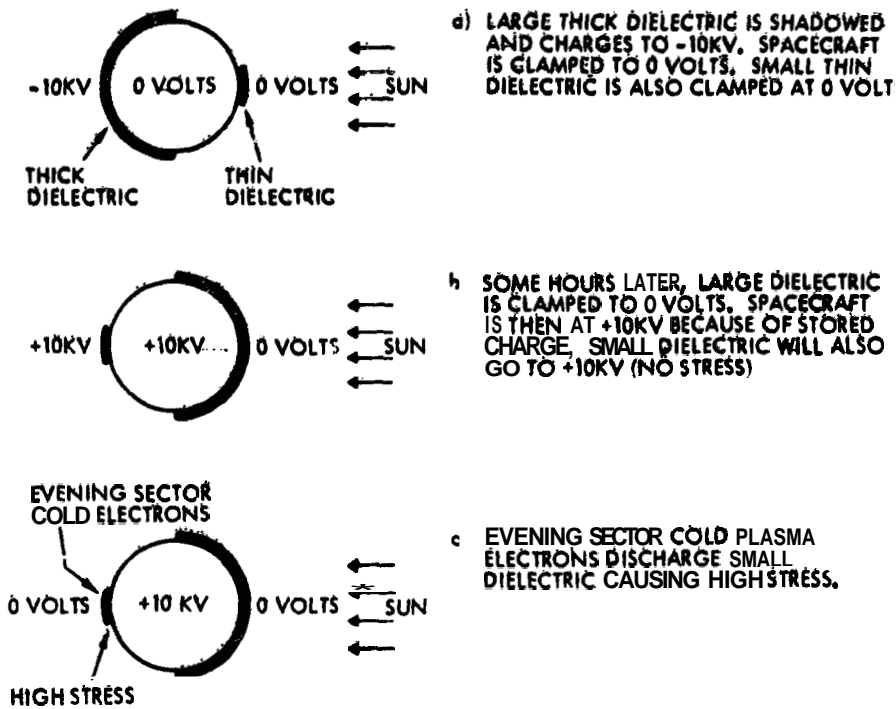


Figure 10. Hypothetical Mechanism for Generation of Afternoon/Evening Time Sector Arc Discharges

The "T" and "C" anomaly distributions suggest that a combination of environmental and spacecraft configuration/orientational factors are at work. The occurrence of afternoon to evening events requires further discussion since the environment in these sectors is not conducive to spacecraft charging. In the paper on spacecraft charging models, it was pointed out that much of the outer dielectric surface materials were very good insulators and that leakage time constants could be in the order of several days. With this charge storage mechanism, it is possible to conceive of configurations in which sunlight applied to a dielectric surface in the late afternoon could cause an increased stress and resulting arc discharge at that time. It is also possible for an enhanced cold plasma environment such as the afternoon/evening detached plasma sector and plasmopause bulge described by Chappell et al¹¹ to selectively reduce the potential of a surface and to therefore cause it to arc. Figure 10 shows diagrammatically how the delayed arc discharges could occur.

5. CORRELATION WITH THE DAY OF THE WEEK

Figure 11 shows the distribution of the days of occurrence of anomalous events according to the day of the week. Separate distributions for the individual types as well as for all of them together are shown. The latter shows a peak on Saturday and Sunday which is about three times the midnight minimum. Individually, the "T" and "C" anomalies also show a weekend peak, but the midweek dips are more nearly a half of the weekend peak, and the transitions from day-to-day are not as smooth as for the composite graph. The "S" anomalies of which there were only four, are about as evenly distributed as they could be. On obtaining this surprising result, the distribution of Fredericksburg and Anchorage A-Indices over the entire period was computed. The results shown in Figure 12 have a maximum variability of 7 percent about the mean. A Friday or Saturday peak in activity is evident but the ratio of maximum to minimum is far less than for the anomalies.

Discussions with E. L. Scarf resulted in one possible explanation. He suggested that a reduced loading of the Canadian power system on weekends might be contributing to the selective depletion of the energetic particle population at geosynchronous altitudes. Helliwell et al¹² have described magnetospheric FLF waves which are induced by the Canadian power system. They point out that VLF radiated powers of less than 10 W could cause noticeable magnetospheric signals and that harmonics of the 1000 MW load of the Alcan Aluminum refineries should radiate considerably more power. Fraser-Smith¹³ has analyzed many years of geomagnetic data and has concluded that an approximately 4 percent enhancement exists in the A_p index on weekends, "which may reasonably be associated with the fact that power consumption is lower (by 30 percent) on weekends." An alternative possibility that has been discussed with the spacecraft operational engineer is the possibility of increased (or decreased) payload usage on weekends resulting in thermal power dissipation effects. The differential usage as well as thermal effects are stated to not having been noticeably dependent on the day of the week, although they have not been looked at in detail with the weekend effect in mind.

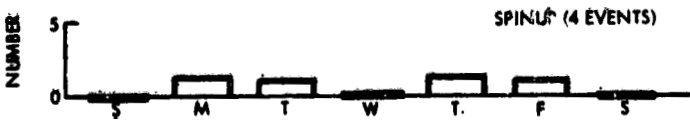
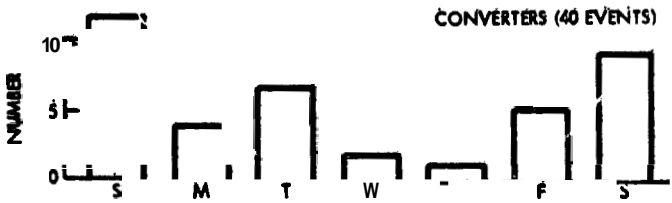
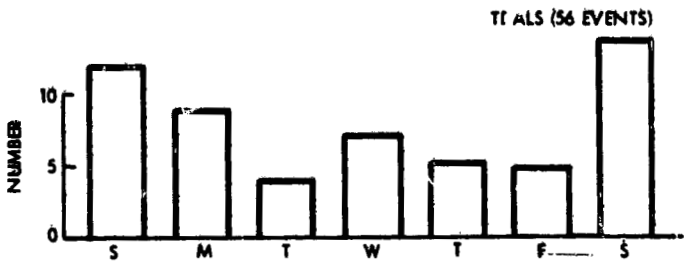
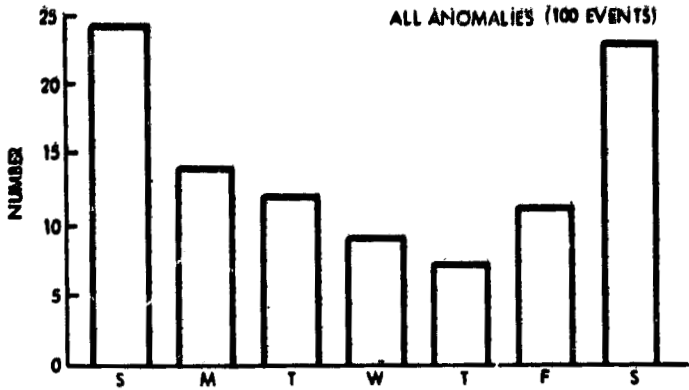


Figure 11. Distribution of Anomalous Events on DSCS Flights 3/4 With Day of the Week

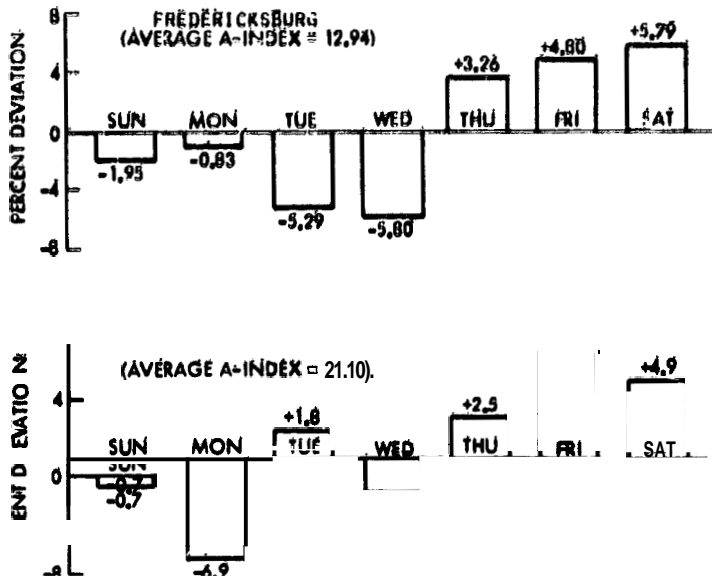


Figure 12. Percent Deviation From Average A-Indices, November 1973-September 1976

6. LONG TERM AND PROGRESSIVE EFFECTS

The most prominent feature of Figures 3-5 is that the frequency of occurrence of anomalies has been decreasing drastically with time. Figure 13 shows the Fredericksburg A-Index smoothed and on a more compressed time scale covering the entire 33 month period since launch. The trend seems to be consistent with the sunspot cycle in that 1974 was in a decreasing phase, and 1976 is near the sunspot minimum. In this sense, the decrease in the number of anomalies might be correlated to the decrease in geomagnetic activity. Reference to Figure 6(c), however, shows that the amount of decrease in average A-Index, coupled with the fact that actual day-to-day variability is much greater than any longer term average, does not account for the decrease in the number of anomalies.

Results of laboratory experiments, of which Figure 14 from Hoffmaster, Inouye and Sellen¹⁴ is an example, show that there are many long term and progressive effects which could account for decreasing rate of anomaly occurrences. Figure 14 shows the hysteretic effect of high energy particle bombardment in reducing bulk conductivity. Another feature observed in laboratory tests is the burnoff of thin films of vacuum deposited aluminum on thermal blankets and second surface mirrors with each arc discharge. It is possible for the increased spark gap length to gradually increase the arc breakdown threshold or for the carbonized

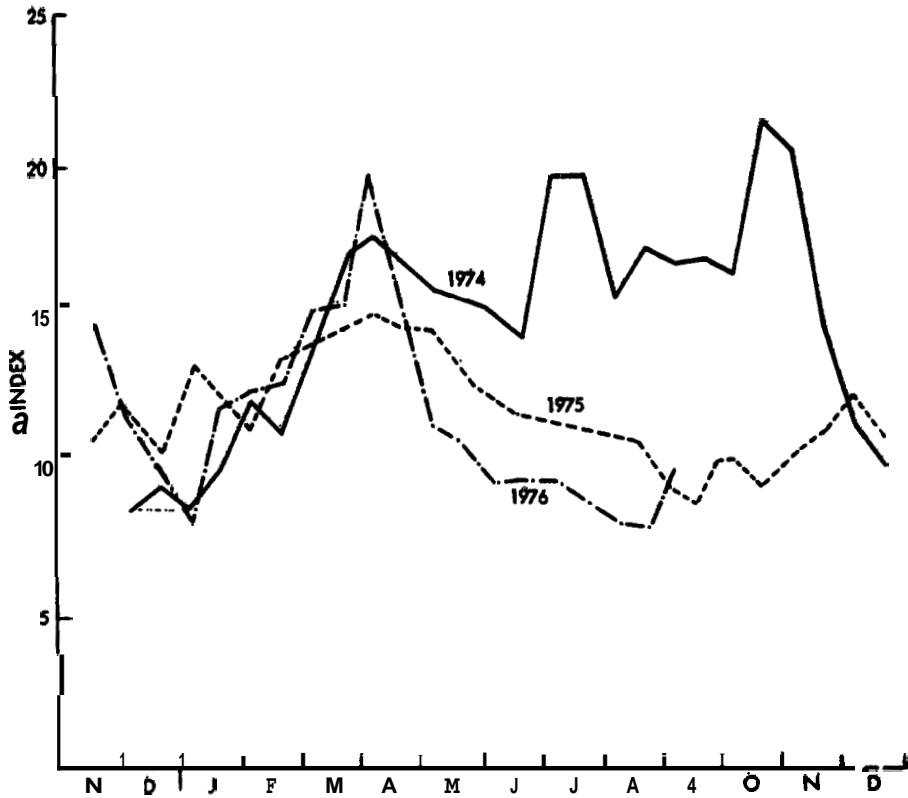


Figure 13. Fredericksburg A-Index Smoothed to Show Yearly Changes

material to decrease the threshold for succeeding discharges. From the view-point of an electrical circuit designer, thin film conductors are extremely poor devices because they are difficult to connect to and are electrically unstable in terms of point-to-point resistance from handling and crinkling. Thermal and ultraviolet irradiation degradation effects on breakdown threshold have not been investigated. Many other long term effects on material and surface characteristics such as photoemission and secondary emission need to be studied. Our view is that these long term and progressive degradation effects are the cause of the long term decrease in the occurrence of anomalous events.

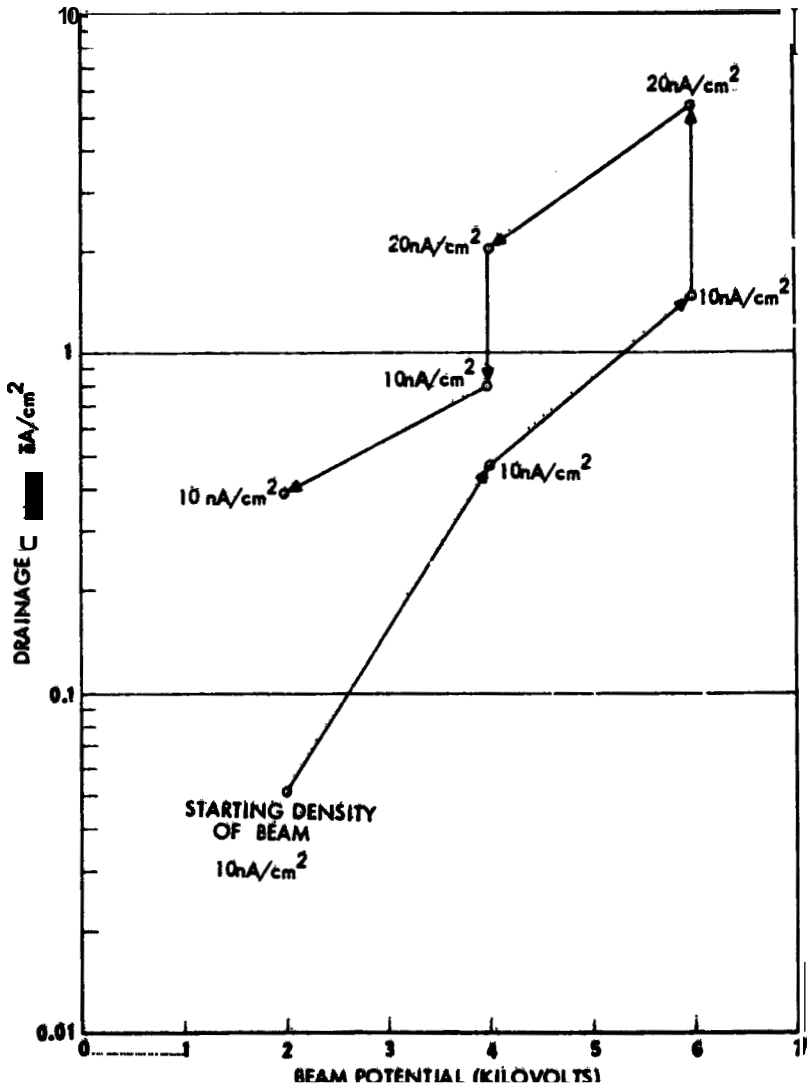


Figure 14. Electron Drainage Current Density as a Function of Electrode Beam Acceleration Voltage for Deposition Flux Densities of 10 nA/cm^2 and 20 nA/cm^2

7. SUMMARY AND CONCLUSIONS

The anomalous events occurring on the DSCS II Launch 2 satellites have been studied with a view towards understanding their causes and initiating countermeasures to eliminate them on future spacecraft. The work presented here underscores the studies of many areas which must be implemented towards achievement of enough information to be able to design spacecraft which are able to withstand the geosynchronous orbit environment.

A basic problem addressed here is whether and how these anomalies are related to the environment. The correlation of the "S" type anomalies with the environment seems quite clear from the A-Index, the local time of occurrence and the equinox season of occurrence. The A-Index correlation of the other types of anomalies was shown to be dubious. Consistency was shown for the other types of anomalies with analytical model predictions of seasonal dependence and location on the spacecraft. The local time distribution of "T" and "C" type anomalies while not meeting the midnight/dawn criterion are, statistically speaking, not inconsistent with an environmental forcing function. The question of why events do not occur in any correlated fashion on two ostensibly identical satellites as close as 10° or as far apart as 180° in longitude has been discussed. Both environmental and/or uncontrolled spacecraft differences are possible sources of the observations. Capacitive energy storage in the outer dielectric surfaces makes it possible to postulate means whereby arc discharges could occur outside the midnight/dawn local time sector. The peak on weekends of the distribution of events on a day-of-the-week basis is a surprising result which may or may not be related to the environment. Finally, the long term decrease in the frequency of occurrence of anomalous events does not seem to be directly related to the environment but rather to on-board progressive and long term degradation effects. In addition to the need for much further work, the conclusion is inescapable that in-flight spacecraft charging/discharging monitors would be an invaluable adjunct to the house-keeping telemetry system of every geosynchronous satellite.

Acknowledgments

This work presented here was performed at TRW under Air Force Contract No. FO 4701-69-C-0091. The author acknowledges the many informative and helpful discussions with members of the Space Sciences Department under A. Rosen, E. W. Greenstadt, N. L. Sanders, and F. I. Scarf; J. Durschinger and R. Alborn of the DSCS II Project office for spacecraft detail, and operation, and Mrs. B. Benefield for typing, assembling and correcting the manuscript.

References

1. Rosen, A., Fredricks, R. W., Inouye, G. T., Sander, N. L., Scarf, F. I., Greenstadt, E. W., Vogl, J. L., and Sellen, J. M., Jr. (1972) Final Report RGA Analysis: Findings Regarding Correlation of Satellite Anomalies With Magnetospheric Substorms, and Laboratory Test Results, TRW Defense and Space Systems 09670-7020-R0-00.
2. Final Report TDAL Gain State Analysis (1973) TRW Defense and Space Systems 09670-7040-RU-00.
3. Final Technical Report Program 777 Anomaly Investigation for Satellites 9433 and 9434 (1974) (3 volumes) TRW Defense and Space Systems 09670 RFP 050-01.
4. Final Report. Performance Anomaly Flight 9431 (1973) TRW Defense and Space System; 24512-AH-006-01.
5. Final Technical Report Program 777 Anomaly Investigation for Satellite 9434 Converters (1975) July-October 1975, TRW Defense and Space Systems 26722-AR-008-01.
6. Rosen, A. (1976) Spacecraft charging: environment induced anomalies, 3. Spacecraft and Rockets, 13:129-136.
7. Inouye, G. T. (1976) Spacecraft potentials in a substorm environment, in Spacecraft Charging by Magnetospheric Plasmas, Alan Rosen, Editor, Vol. 47 Progress in Astronautics and Aeronautics., MIT Press, pp. 103-120.
8. Fredricks, R. W., and Scarf, F. I. (1973) Observations of spacecraft charging effects in energetic plasma regions, in Photon and Particle Interactions with Surfaces in Space, R. J. L. Crand, Editor, D. Reidel Pub. Co., Dordrecht-Holland, pp. 277-308.
9. Lyons, L. R., Thorne, R. M., and Kennel, C. F. (1972) Pitch angle diffusion of radiation belt electrons within the plasmasphere, J. Geophys. Res., 77:3455-3474.
10. Inouye, G. T. (1975) Spacecraft charging model, J. Spacecraft and Rockets 22:613-620.
11. Chappell, C. R., Harris, K. K., and Sharp, G. W. (1971) The dayside of the plasmasphere, J. Geophys. Res. 76:7632-7647.

12. Hellwell, R. A., Katsufakis, J. P., Bell, T. F., and Raghuram, R. (1975) VLF line radiation in the earth's magnetosphere and its association with power system radiation, J. Geophys. Res. 80:4249-4258.
13. Fraser-Smith, A. (1976) to be published.
14. Hoffmaster, D. K., Inouye, G. T., and Sellen, J. M. Jr. (1976) Surge current and electron swarm tunnel tests of thermal blanket and ground strap materials, TRW Defense & Space Systems 76, 4351. 1-103, also presented at USAF/NASA Spacecraft Charging Technology Conference.

Appendix A.

DSCS-II S/C 9433 and 9434 Anomalous Events

<u>Event No.</u>	<u>S/C Event No.</u>	<u>Type No.</u>	<u>Date</u>	<u>Day</u>	<u>Day</u>	<u>GMT</u>	<u>Local Time</u>	<u>Comments</u>
Launch	*****	-----	12-13-73	1	THU	----	-----	Launch
1	9434-1	T-1	12-22-73	10	SAT	1653	09.21	Both S/C at initial positions 12-21-73
2	9433-1	T-2	12-24-73	12	MON	0348	20.80	-
3	9434-2	T-3	12-25-73	13	TUE	0121	17.68	-
4	9433-2	T-4	12-25-73	13	TUE	----	03.42	0900-1150 GMT
5	9433-3	RCA	12-29-73	17	SAT	0108	18.13	Only RGA event
6	9434-3	T-5	12-29-73	17	SUN	2224	15.08	-
7	9433-4	T-6	1-2-74	21	WED	1114	04.23	-
8	9434-4	1-7	1-3-74	22	THU	0731	23.85	-
9	9434-5	T-8	1-11-74	30	FRI	1621	08.68	-
10	9433-5	T-9	1-12-74	31	SAT	0008	17.13	-
11	9433-6	T-10	1-19-74	38	SAT	1726	10.43	S/C 9433 starts moving 1-23-74
12	9434-6	1-11	1-26-74	45	SAT	1023	02.71	-
13	9433-7	1-12	1-27-74	46	SUN	0705	01.41	-
14	9434-7	1-13	1-30-74	49	WED	0745	00.08	S/C 9434 starts moving 1-30-74
15	9433-8	1-14	2-1-74	51	FRI	0757	03.10	-
16	9433-9	T-15	2-12-74	62	TUE	0958	06.95	-
17	9433-10	1-16	2-17-74	67	SUN	0936	07.41	Both S/C at final positions 3-1-74
18	9433-11	1-17	4-7-74	116	SUN	--	08.97	0710-1230 GMT
19	9433-12	T-18	4-9-74	118	TUE	--	08.75	0700-1215 GMT
20	9433-13	T-19	4-10-74	119	WED	--	08.58	0644-1210 GMT
21	9434-8	1-20	4-25-74	134	THU	--	19.19	1716-2251 GMT
22	9434-9	1-21	6-27-74	197	THU	--	05.38	1420-2105 GMT

<u>Event No.</u>	<u>S/C Event No.</u>	<u>Type No.</u>	<u>Date</u>	<u>Day No.</u>	<u>Day</u>	<u>GMT</u>	<u>Local Time</u>	<u>Comments</u>
23	9434-10	C-1	7-18-74	218	THU	0505	16.75	First Converter Anomaly
24	9434-11	T-22	7-20-74	220	SAT	1800	05.67	-
25	9434-12	T-23	7-20-74	220	SAT	2130	09.17	-
26	9434-13	T-24	7-27-74	227	SAT	0305	15.75	-
27	9434-14	C-2	8-17-74	248	SAT	1418	01.97	-
28	9434-15	C-3	8-17-74	248	SAT	1819	05.98	-
29	9434-16	C-4	8-17-74	248	SAT	1819	05.98	1819.3 GMT
30	9434-17	C-5	8-17-74	248	SAT	1832	06.20	-
31	9434-18	C-6	8-17-74	248	SAT	1859	06.65	-
32	9434-19	T-25	8-18-74	249	SUN	1040	22.33	-
33	9434-20	T-26	8-18-74	249	SUN	1139	23.32	-
34	9434-21	T-27	8-18-74	249	SUN	1139	23.32	1139.4 GMT
35	9434-22	T-28	8-18-74	249	SUN	1325	01.08	-
36	9434-23	T-29	8-18-74	249	SUN	1515	02.92	-
37	9434-24	C-7	8-18-74	249	SUN	1600	03.67	-
38	9434-25	C-8	8-18-74	249	SUN	1640	04.33	-
39	9434-26	C-9	8-18-74	249	SUN	1644	04.40	-
40	9434-27	T-30	8-24-74	255	SAT	--	17.03	0225-0846 GMT
41	9434-28	T-31	8-24-74	255	SAT	--	22.62	0820-.344 GMT
42	9434-29	C-10	8-24-74	255	SAT	1830	06.17	-
41	9434-30	C-11	9-3-74	265	TUE	2106	08.77	-
44	9434-31	C-12	9-1-74	265	TUE	2256	10.60	-
45	9434-32	S-1	9-20-74	282	FRI	1330	01.17	First Spinup Anomaly
46	9434-33	T-32	9-23-74	285	MON	0446	16.33	-
47	9434-34	S-2	9-26-74	288	THU	1512	02.87	-
48	9434-35	S-3	10-1-74	293	TUE	1721	05.02	-
49	9434-36	T-33	10-2-74	294	WED	1706	04.77	-

<u>Event No.</u>	<u>S/C Event No.</u>	<u>Type No.</u>	<u>Date</u>	<u>Day No.</u>	<u>Day</u>	<u>GMT</u>	<u>Local Time</u>	<u>Comments</u>
50	9434-37	t-34	10-7-74	299	MON	2230	10.17	-
51	9434-38	T-35	10-11-74	303	FRI	2225	10.08	-
52	9434-39	T-3b	10-12-74	304	SAT	1420	02.00	-
53	9434-40	7-37	10-14-74	306	MON	0539	17.32	-
54	9434-41	C-13	10-14-74	306	MON	1550	03.49	-
55	9434-42	C-14	10-14-74	306	MON	1557	03.62	-
56	9434-43	T-38	10-14-74	306	HON	1741	05.35	-
57	9434-44	S-4	10-14-74	366	MON	2013	07.88	Last Spinup Anomaly
58	9434-45	C-15	10-18-74	310	FRI	2359	11.35	-
53	9434-46	C-16	10-19-74	311	SAT	0008	11.80	-
60	9434-47	C-17	10-22-74	314	TUE	2310	10.83	-
61	9434-40	C-18	10-22-74	314	TUE	2330	11.17	-
62	3434-49	T-39	10-23-74	315	WED	0543	16.72	-
63	9434-50	T-40	10-24-74	316	THU	0415	15.92	-
64	9434-51	C-19	11-3-74	326	SUN	2114	00.90	-
65	9434-52	C-2u	11-4-74	327	HON	1140	23.33	-
66	9434-53	C-21	11-4-74	327	MON	1508	02.08	switched \approx 57 times
67	9434-54	C-22	11-8-74	331	FRI	0810	19.83	-
68	9434-55	C-23	11-8-74	331	FRI	1015	22.17	-
69	9434-56	C-24	11-9-74	332	SAT	0510	16.83	-
70	9434-57	C-25	11-9-74	332	SAT	0655	18.58	-
71	9434-58	C-26	11-10-74	333	SUN	1756	05.60	-
72	9434-59	C-27	11-10-74	333	SUN	2005	07.75	-
73	9434-60	T-41	11-16-74	339	SAT	1219	23.98	-
74	9434-61	C-28	11-17-74	340	SUN	1645	04.42	-
75	9434-62	C-29	11-17-74	340	SUN	1927	07.12	-
76	9434-63	i-42	11-18-74	341	MON	0025	12.08	-

<u>Event No.</u>	<u>S/C Event No.</u>	<u>Type No.</u>	<u>Date</u>	<u>Day No.</u>	<u>Day</u>	<u>GMT</u>	<u>Local Time</u>	<u>Comments</u>
77	9434-64	T-43	11-20-74	343	WED	1030	22.19	-
78	9434-65	C-30	11-22-74	344	FRI	1003	21.72	-
79	9434-66	C-31	11-22-74	345	FRI	1200	00.33	-
80	9434-67	T-44	11-24-74	347	SUN	1935	07.25	-
81	9434-68	T-45	11-25-74	348	MON	2201	09.68	-
82	9434-69	C-32	11-27-74	350	WED	1701	04.68	-
83	9434-70	C-33	11-27-74	350	WED	1943	07.38	-
84	9434-71	C-34	12-1-74	354	SUN	0052	12.67	-
85	9434-72	C-35	12-1-74	354	SUN	0512	16.87	-
86	9434-73	C-36	12-10-74	363	TUE	0008	11.80	-
87	9434-74	C-37	12-10-74	363	TUE	0125	13.08	-
88	9434-75	C-38	12-10-74	363	TUE	0305	14.75	-
89	9434-76	1-46	12-14-74	367	SAT	6652	18.53	-
90	9434-77	C-39	12-15-74	368	SUN	1909	06.82	-
91	9434-78	C-40	12-15-74	368	SUN	NA	NA	Switched 6 times. Last converter anomaly.
92	9434-79	T-47	1-6-75	390	MON	0355	15.58	
93	9434-80	Gimbal-1	3-12-75	455	WED	NA	NA	Gimbal anomaly only
94	9434-81	Gimbal-2	3-14-75	457	FRI	1459	02.65	Gimbal anomaly only
95	9433-14	t-48	3-31-75	474	MON	1021	22.02	S/C 9433 anomaly
96	9434-82	T-49	10-5-75	662	SUN	0055	12.58	
97	9434-83	T-50	10-10-75	667	FRI	0035	12.25	-
98	9434-84	1-51	10-12-75	669	SUN	0013	11.88	-
99	9434-85	T-52	11-6-75	694	THU	1527	03.12	-
100	9434-86	1-53	11-3-75	697	SUN	0357	15.62	Last anomaly as of 8-23-76